



Inorganic binder-containing composite cathode contact materials for solid oxide fuel cells

Michael C. Tucker^{a,*}, Lei Cheng^a, Lutgard C. DeJonghe^b

^aEnvironmental Energy Technology Division, Lawrence Berkeley National Laboratory, 1 Cyclotron Rd, Berkeley, CA 94720, USA

^bMaterials Sciences Division, Lawrence Berkeley National Laboratory, 1 Cyclotron Rd, Berkeley, CA 94720, USA

HIGHLIGHTS

- ▶ Addition of inorganic binder to SOFC contact materials enhances bonding.
- ▶ Enhanced bonding after low-temperature cure.
- ▶ Acceptably low ASR achieved for select binder compositions.

ARTICLE INFO

Article history:

Received 20 August 2012

Received in revised form

27 September 2012

Accepted 29 September 2012

Available online 9 October 2012

Keywords:

Solid oxide fuel cell

Cathode contact material

Inorganic binder

Stainless steel interconnect

ABSTRACT

The feasibility of adding inorganic binder to conventional SOFC cathode contact materials in order to improve bonding to adjacent materials in the cell stack is assessed. A variety of candidate binder compositions are added to LSM. The important properties of the resulting composites, including ASR, reactivity, and adhesion to LSCF and MCO-coated 441 stainless steel are used as screening parameters. The most promising CCM/binder composites are coated onto MCO-coated 441 coupons and anode-supported button cells with LSCF cathode, and tested at 800 °C. It is found that a LSM-644A composite displayed excellent initial performance and promising stability. Indeed, addition of binder is found to improve bonding of the CCM layer without sacrificing CCM conductivity.

© 2012 Elsevier B.V. All rights reserved.

1. Introduction

Assembly of solid oxide fuel cell (SOFC) stacks typically involves mechanically and electrically connecting a number of cells and interconnects in series. Connection of the cathode to the interconnect (or coating on the interconnect) is usually accomplished by compression of the stack using an external load frame, and is often aided by the use of a cathode contact material (CCM). The CCM is an electrically conductive material, and is applied as a paste or ink during stack assembly to form a continuous layer or discrete contact pads. The CCM provides electrical connection between the cathode and interconnect, and can also serve to improve in-plane conduction over the area of the cathode. Fig. 1 indicates placement of the CCM in the fuel cell stack. Often, the CCM is simply a thick layer of the electrocatalyst used in the cathode. [1] For example, a thin LSM-YSZ cathode layer optimized for electrochemical activity can be covered with a thick LSM CCM layer optimized for gas transport and electrical conductivity. A significant limitation of this approach,

however, is that most cathode compositions require firing at high temperature (>1100 °C) to achieve good sintering. [2] The use of ferritic stainless steel as the interconnect material limits the firing temperature to 1000 °C or lower. In practice, therefore, using a cathode catalyst CCM in conjunction with a stainless steel interconnect results in low CCM layer strength and minimal adhesion at the CCM/interconnect or CCM/cathode interface.

Efforts to decrease the required sintering temperature through doping [3], control of the defect structure [3,4], and addition of glass [5] have had some success. In the present work, we assess the merit of adding inorganic binder to the CCM in order to improve bonding without sacrificing acceptable conductivity of the resulting binder-ceramic composite.

2. Approach

The CCM composition must fulfill the following requirements:

- high electronic conductivity
- sintering/bonding at 1000 °C or lower
- good CTE match to other cell components

* Corresponding author. Tel.: +1 510 486 5304; fax: +1 510 486 4881.

E-mail address: mctucker@lbl.gov (M.C. Tucker).

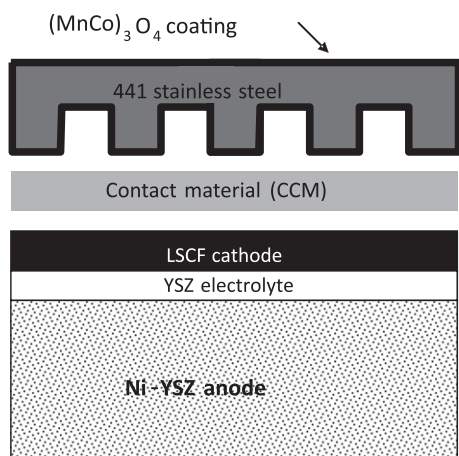


Fig. 1. Schematic representation of CCM placed between SOFC cell and coated stainless steel interconnect.

- mechanical strength within the CCM layer and at the interfaces to cathode and interconnect

Our approach is to fabricate composite mixtures of SOFC cathode material and inorganic binder. Conventional CCM pastes use a cathode material to achieve both bonding and electrical contact. In contrast, the approach we take is to separate the functions of electrical contact and mechanical (or chemical) bonding. Inorganic binders are frequently used in the manufacture of high-temperature adhesives, mortars, plasters, and cements. Ceramic–inorganic binder composites are widely used as seals for SOFCs, because they wet to other SOFC materials and bond after curing at relatively low temperature (often room temperature to about 350 °C), producing mechanically robust seals. [6] For example, SOFC ceramic adhesive sealants typically comprise alumina or zirconia filler particles and a polyphosphate-, silicate-, or aluminosilicate-based inorganic binder suspended or dissolved in water. The binder functions by crosslinking, polymerization, or curing various polyphosphate, polysialate, polysiloxo, poly(sialate–siloxo), silicate etc. groups. The adhesive may be applied as a wet paint or paste, and hardens and cures upon drying or heating. The heating temperature (if any) is much lower than the temperature required to sinter the ceramic filler particles. For example, alumina requires >1500 °C to sinter, but alumina-filled ceramic adhesive can be cured at <400 °C to produce a hard, dense, well-adhered coating or bonding layer. Such adhesives are commercially available from Aremco and Cotronics (exemplary products include 552T, 503T, 644A, 644S, 830, 542, 794, 795, 797). The goal is to prepare a CCM composition that displays improved bonding via addition of inorganic binder, without sacrificing conductivity or long term stability of the resulting mixture.

Initially, single commercially-available inorganic binders are mixed with LSM. These mixtures are characterized for conductivity, mechanical properties, and reaction between the LSM and binder. The most promising binder/LSM mixtures are applied to MCO-coated 441 steel coupons and tested for area-specific resistance (ASR). Those mixtures showing the best ASR are then applied to button cells with Pt mesh current collectors and operated at 800 °C to determine performance and stability.

3. Experimental methods

3.1. Materials

LSM powder was purchased from Praxair. Aqueous inorganic binder solutions were purchased from Aremco (542, 830, 644A,

644S, 552T) and Cotronics (794, 795). Metal powders were supplied by Ametek (434), Novamet (316 flakes, dendritic Ni 525), and Alfa Aesar (NiCr).

3.2. XRD and SEM

XRD (Philips X'Pert) was used to check reaction between binder and LSM. The XRD trace for pure LSM was compared to those for mixtures of LSM and binders after curing at 360 °C, and after sintering at 1000 °C for 1 h in air. Powders and ASR specimens were imaged with SEM (Hitachi S4300SE/N).

3.3. Paste fabrication and initial assessment

Metal or LSM (1000 °C coarsened) powders were mixed with the amount of each binder required to make a workable paste (typically 4 g powder and ~1.5 g aqueous binder solution). The pastes were then applied to an alumina substrate, cured according to the manufacturers' instructions (typically 360 °C), and heated to 800 °C for 2 h. Upon cooling, the resistance was estimated with a multi-meter, and the bonding was qualitatively assessed by scraping the cement with a blade. In certain cases, load at failure was determined using stud-pull tests, described below.

3.4. ASR measurements

Specimens for ASR measurements were prepared according to the geometry in Fig. 6. Various CCM inks were prepared by mixing the powders with aqueous inorganic binder solutions using a planetary mixer (Thinky). 441 stainless steel coupons were coated with MCO by screenprinting at Pacific Northwest National Laboratory (PNNL). CCM layers were then brush painted onto the MCO layer, dried under a heat lamp and cured in air at according to the manufacturers' instructions (typically 360 °C), followed by a 1 h hold at 800 °C. Pt paste (Heraeus CL11-5349) and Pt mesh (Alfa Aesar 10283) were applied as current collectors on the CCM layers, and sintered at 800 °C. Pt mesh was spot-welded to the 441 coupon. The ASR specimens were then subjected to 500 mA current for 200 h at 800 °C in air. DC current was applied in a 4-probe configuration using a Biologic VMP3 potentiostat.

3.5. Mechanical analysis

Interfacial adhesion was assessed using an epoxy-stud pull tester (Quad Group Sebastian V). CCM/binder pastes were printed and sintered onto LSCF-coated YSZ disks and MCO-coated 441 coupons.

3.6. Cell testing

Anode supported button cells with LSCF cathode and GDC barrier layer (MSRI) were used. The cathode was coated with CCM paste and then cured as above. Pt mesh current collector was attached with Pt paste (Heraeus) to both the anode and CCM (or bare LSCF cathode in the case of no-CCM baseline cells). The cells were mounted to alumina tubes with Aremco 552 sealant and tested at 800 °C with 97%H₂/3%H₂O fuel. After obtaining initial impedance spectra, the cells were operated at 300 mA cm⁻² for roughly 250 h. DC current was applied in a 4-probe configuration using a Biologic VMP3 potentiostat.

4. Results and discussion

4.1. Proof of concept: metal-binder composites

Aremco 552 is a common SOFC sealant, containing alumina filler particles and aqueous sodium silicate binder. Alumina-free thinner

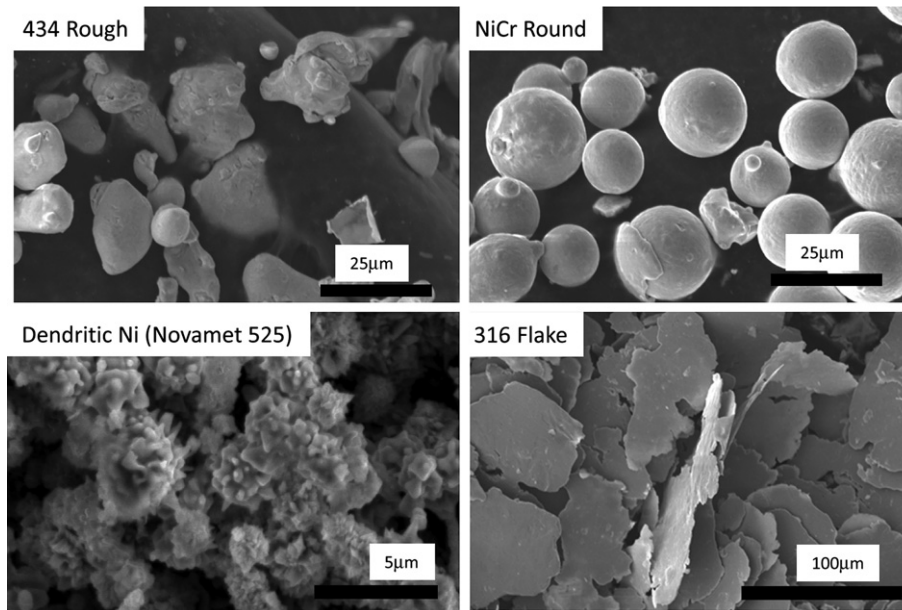


Fig. 2. SEM images of various metal powders used in this work.

(binder and water) is available as 552T. Mixtures of metal particles and 552T were prepared to assess the general behavior of a well-studied SOFC inorganic binder upon replacement of the alumina filler with conductive particles. A variety of metal particle types were used to determine the effect of particle shape, surface area, surface roughness, etc. on suitability as a conductive additive. Images of the metal particles are shown in Fig. 2. The particles were mixed with 552T at a loading ratio that provided a workable paste. The paste was then brushed onto an alumina substrate, cured, and tested for resistance and load at failure. The results are shown in Table 1. Pastes including the flake and round particles did not bond to the substrate. All composites were insulating (i.e. the metal particles were not contacting well enough to provide a percolating network), except for dendritic nickel with displayed good conductivity. Note that the dendritic nickel is significantly smaller and rougher than the other particle shapes. Fig. 3 shows results for 552T/dendritic nickel over a range of filler ratios. Strength and conductivity generally increased with increasing Ni content, and at high Ni loading (~63 wt%), a very strong bond and low resistivity was achieved. Although Ni is of course not a viable option due to oxidation at operating temperature, these results were very encouraging in that they indicated that a binder/conductor mixture that displays good bonding and high conductivity can be prepared, and therefore the concept was worth pursuing further.

4.2. Screening various binder compositions

Based on the observation above that a small, rough particle provided the best results, we proceeded to produce cement pastes filled with LSM particles. Initial trials used sub-micron particles as-

Table 1
Summary of results for pastes made with metal powders and 552T binder.

Metal type	Metal shape	Paste solids content (wt%)	Resistance (Ohms)	Load at failure (Mpa)
316 steel	Flake	33	Off-scale	No bonding
NiCr	<15 µm sphere	77	Off-scale	No bonding
434 stainless	<25 µm rough	68	Off-scale	2
Ni	<5 µm dendritic	50	<5	3

received from Praxair, and pastes with 50 and 63 wt% LSM were prepared. Unfortunately, they cracked during drying, presumably from drying stress associated with the very high surface area of the particles. We therefore coarsened LSM to reduce surface area. Images of the LSM particles after coarsening at various temperatures are shown in Fig. 4. We chose to proceed with particles coarsened at 1000 °C (reduced surface area, but still sub-micron particle size and rough like dendritic nickel) and 1300 °C (greatly increased particle size). Pastes produced with the 1300 °C particles were not very conductive after curing. The 1000 °C-particles provided good conductivity, and the surface area had been reduced sufficiently to avoid drying-stress cracks. The rest of the work reported here used LSM pre-coarsened at 1000 °C.

Many aqueous inorganic binder systems are available commercially. We selected promising candidates from Aremco and Cotronics. It is known that alkali metals and alkaline earth metals can interact with stainless steel (or other Cr-containing materials) to form volatile compounds containing Cr. In fact during our initial work with 552T/LSM mixtures, we noted the formation of a Na–Cr–O compound (presumably Na_2CrO_4) in the CCM layer adjacent to a stainless steel substrate. The presence of these compounds in the cathode air supply can deposit Cr within the porous cathode, thereby degrading fuel cell performance when using a cathode composition that is not tolerant to the presence of Cr [7]. It is therefore desirable to use a bonding agent composition that does not contain significant amounts of alkali metals and alkaline earth metals (K, Na, Ca, Sr, etc) when used in conjunction with LSM, LSCF, or other cathode materials that are degraded by Cr. Table 2 lists the binders selected via this criteria, none of which contained alkali or alkaline earth metals as determined via SEM/EDAX.

Each of these binder candidates was mixed with LSM powder, printed onto alumina substrate and cured. After curing, the room temperature resistance and bond strength were qualitatively assessed. Based on these observations, 830, 542, and 644A were selected as the most promising candidates for further testing. Note that some reaction between 542 and LSM was observed during mixing. The pH of 542 is quite low, and we noted slight evolution of gas and dissolution of LSM upon contacting the powder with the binder, presumably due to acidic attack. This behavior was not observed for the other binders. XRD was used to determine phase

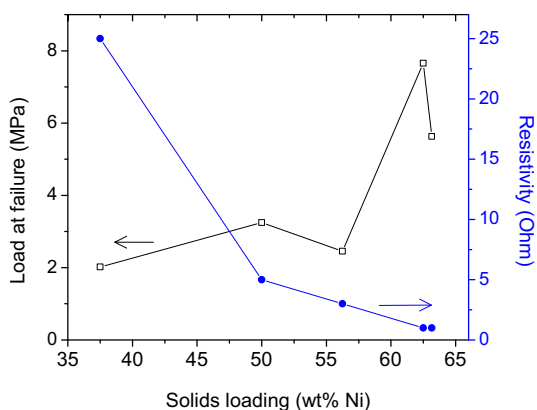


Fig. 3. Pull test and room temperature resistivity of various 552T/dendritic Ni mixtures after curing on alumina substrate.

stability of the LSM after curing, and after exposure to air at 800 °C for 100 h (to mimic conditions during SOFC operation). No change in the XRD traces were observed after curing, but LSM was observed to react with 542 after exposure at 800 °C, as shown in Fig. 5. We were unable to clearly identify the peaks, but presume they arise from a mixture of reaction product phases. We did not rule out 542 as a candidate because if the reaction products are conductive, or improve bonding, the resulting composite may be effective.

Table 2

Summary of screening results for various LSM/binder mixtures.

Binder type	Major components	pH	React with CCM powder?	Room-temp resistance (Ohm)	Bonding to Al ₂ O ₃
542	Al, P, minor Si	2.5	Slight	10 k	OK
794	Al, P	3	NO	100 k	Poor
795	Al, Cl	3.5	NO	10 k	Very weak
644A	Al	4	NO	20 k	Weak
644S	Si	9	NO	200 k	Poor
830	Si, minor S	11.4	NO	20 k	OK

4.3. Mechanical testing of most promising compositions

Adhesion stud pull tests were performed at room temperature to determine the effect of binder addition on CCM intralayer strength and bonding to adjacent materials (LSCF and MCO-coated 441 steel). The results are shown in Table 3. Pure LSM was sintered at 1000 °C (the upper limit of acceptable processing temperature with steel present), and the LSM/binder composites were cured at 360 °C and then exposed to air at 800 °C for 1 h. Addition of each binder improved or maintained the load at failure for both substrate types, relative to pure LSM. Note that adhesion of LSM to LSCF was too weak to be measured. Several specimens were prepared, but all broke during mounting of the specimen in the test fixture. In all other cases, delamination appeared to occur at the interface between the CCM and adjacent material, as opposed to within the CCM. Future efforts to further improve mechanical

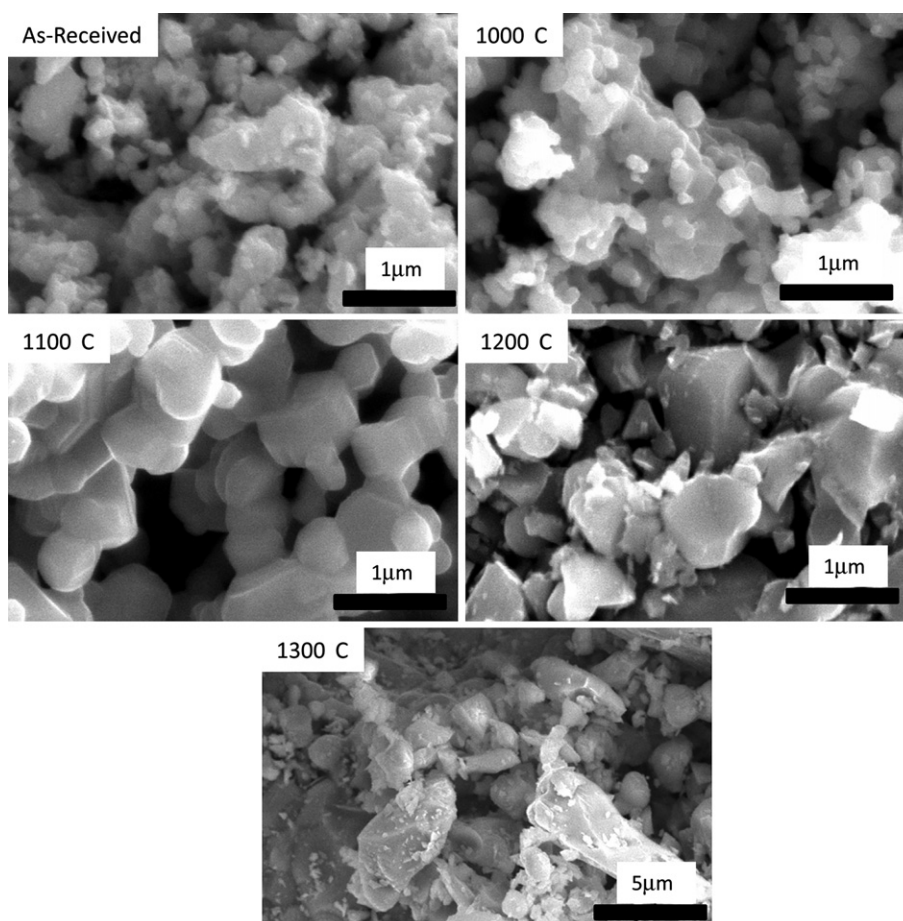


Fig. 4. SEM images Praxair LSM particles after calcining at various temperatures in air.

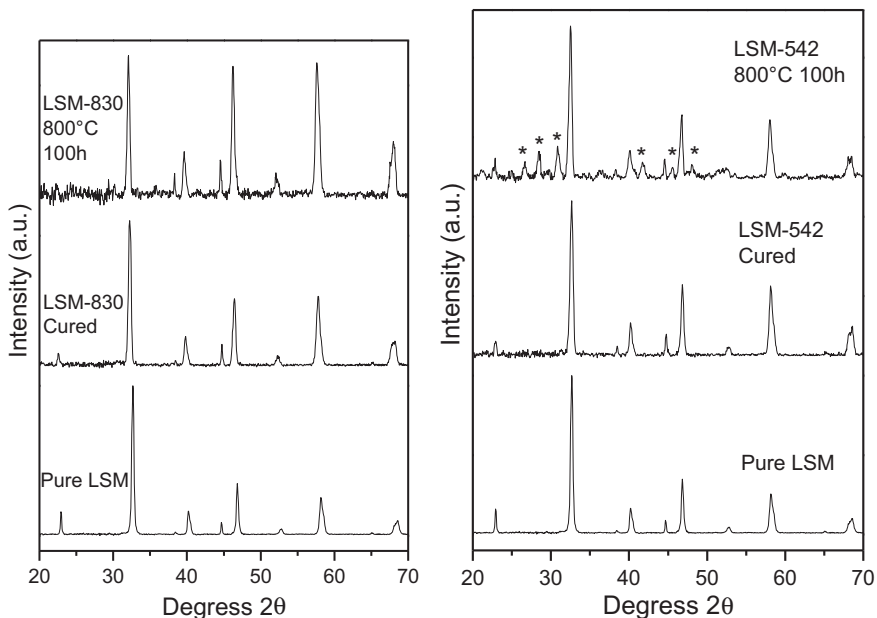


Fig. 5. XRD traces for LSM/830 and LSM/542 after curing and exposure to air at 800 °C for 1 h.

properties of the CCM layer should therefore focus on deposition techniques, surface preparation, and other factors that impact interfacial adhesion.

4.4. ASR results for most promising compositions

The area specific resistance (ASR) for each of the most promising candidates was observed over a period of about 200 h in air at 800 °C, with 500 mA cm⁻² current flowing through the specimen, as shown in Fig. 6. The geometry for the ASR test specimens is shown in the Figure. In our previous work [5], we determined that the LSCF/CCM interface contributed much less to the total ASR than the CCM/MCO/441SS layers, so we only measured the latter in this work. The baseline MCO-coated 441 coupon (no CCM) showed a low initial ASR of about 5 m Ohm-cm², and a small and steady increase over the 200 h testing time, presumably due to chromia scale growth at the MCO/stainless steel interface. The ASR for both LSM/644A and LSM/830 showed similar behavior, although the initial value for LSM/830 was somewhat larger than for the uncoated baseline. The ASR for LSM/542 was unacceptably high. It was an order of magnitude higher than the other candidates, and comparable to the total cell impedance expected for a high-performance cell as shown below in Section 4.5. Thus, we downselected to LSM/830 and LSM/644A for further validation and testing.

Fig. 7 shows a representative polished cross-section image of an ASR specimen after testing. Thin MCO and Cr₂O₃ layers are visible between the stainless steel and CCM layers. The CCM layer is continuous, with some small voids, and well-adhered to the substrate. Some agglomeration is evident in the CCM layer. We presume these agglomerates originated during calcination at

1000 °C, and were not broken up during planetary milling to produce the paste. To determine if these agglomerates affect the electrical properties of the CCM layer, we prepared some specimens in which the coarsened CCM powder was ball-milled or planetary-milled prior to paste production with the aqueous inorganic binder. Although the agglomerates were indeed eliminated by this processing, the initial ASR (tested to 60 h) was unaffected by the change in microstructure (not shown).

4.5. In-situ testing of most promising compositions

The remaining two most promising CCM/binder composites were further subjected to in situ testing on anode-supported

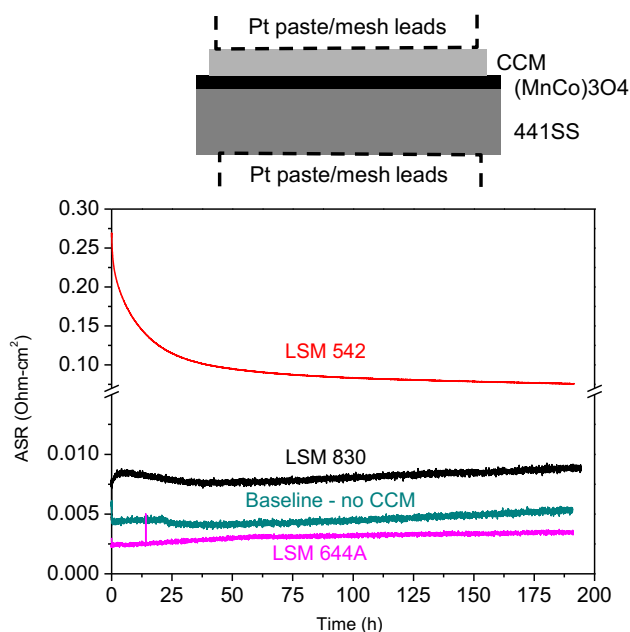


Fig. 6. Schematic of experimental setup and results for ASR testing of various LSM/binder CCM layers on MCO-coated 441 stainless steel substrate.

Table 3
Pull-test results for various LSM/binder mixtures and pure LSM on MCO-coated 441 steel and LSCF-coated YSZ substrates.

Composition	Adhesion on MCO441 (MPa)	Adhesion on LSCF (MPa)
LSM	1.1	0.0
LSM 542	3.1	0.8
LSM 830	1.1	0.5
LSM 644A	1.6	1.1

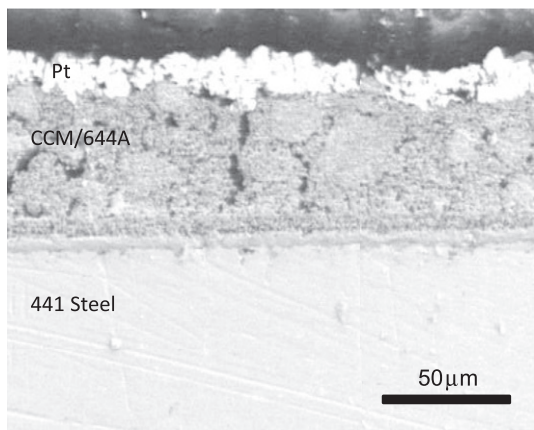


Fig. 7. Cross-section SEM image of ASR specimen after testing.

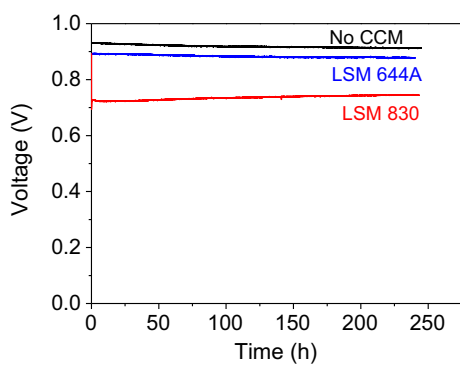


Fig. 8. Performance of anode-supported cells with various CCM layers at 800 °C, 300 mA cm⁻² with moist hydrogen fuel.

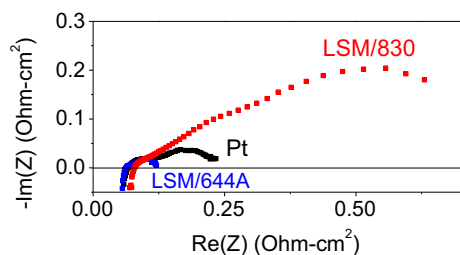


Fig. 9. AC impedance spectra of anode-supported cells with various CCM layers at 800 °C with moist hydrogen fuel.

button cells with LSCF cathode. The CCM candidates (and Pt paste as baseline) were used to bond a Pt mesh current collector to the LSCF. The intention with this arrangement was to determine if the CCM interacted deleteriously with the cathode, causing reduced performance or loss of stability. Indeed, the addition of LSM/830 significantly reduced performance, as shown in Fig. 8. Note this

result was confirmed with a second cell (not shown). The cell with LSM/644A showed slightly lower voltage throughout the operation time than that with Pt paste, however, the difference was stable and the same as the difference in OCV between the two cells. We therefore attribute the lower voltage to seal quality, and not to the presence of LSM/644A. This is consistent with the AC impedance spectra of the cells, shown in Fig. 9. The ohmic impedance of LSM/644A is the same as for Pt paste, and the polarization impedance is somewhat smaller. In contrast, both the ohmic impedance and total impedance are significantly larger for LSM/830. Based on these results, we rejected LSM/830 for further development.

5. Conclusions

The feasibility of adding inorganic binder to conventional CCM materials in order to improve bonding has been assessed. The composition of the inorganic binder plays a significant role in the quality of the resulting composite. Many binders reacted with the CCM or reduced the conductivity of the CCM/binder composite to an unacceptably low level. The binders 644A and 830 minimally increased the ASR of a coated steel substrate, and so were pursued further. Addition of 830 to the CCM layer did, however, adversely affect performance of an operating anode-supported cell. Addition of 644A did not significantly affect cell performance or stability during 250 h operation at 800 °C.

Based on these results, we conclude that addition of inorganic binder to the CCM is an effective strategy to improve bonding and mechanical properties of the resulting CCM/binder composite, without sacrificing acceptable conductivity. Addition of 644A binder to LSM was a particularly satisfying example; adhesion strength was significantly improved, while maintaining a high and stable cell performance. Future work will determine if the improvement in bonding persists at the SOFC operating temperature, and attempt to demonstrate long-term stability in the presence of Cr-containing stainless steel interconnect.

Acknowledgments

This work was supported by the U.S. Department of Energy, National Energy Technology Laboratory and in part by the U.S. Department of Energy under Contract no. DE-AC02-05CH11231. The authors thank Program Manager Joseph Stoffa, and Jeffry Stevenson and Ryan Scott at Pacific Northwest National Laboratory for MCO deposition.

References

- [1] S. Sugita, Y. Yoshida, H. Orui, K. Nozawa, M.u. Arakawa, H. Arai, J. Power Sources 185 (2008) 932–936.
- [2] M.C. Tucker, L. Cheng, L.C. DeJonghe, J. Power Sources 196 (2011) 8313–8322.
- [3] S. Simner, M. Anderson, J. Bonnett, J. Stevenson, Solid State Ion. 175 (2004) 79–81.
- [4] B.P. McCarthy, L.R. Pederson, Y.S. Chou, X.-D. Zhou, W.A. Surdoyal, L.C. Wilson, J. Power Sources 180 (2008) 294–300.
- [5] M.C. Tucker, L. Cheng, L.C. DeJonghe, J. Power Sources 196 (2011) 8435–8443.
- [6] J. Fergus, J. Power Sources 147 (2005) 46–57.
- [7] B.J. Ingram, T.A. Cruse, M. Krumpelt, J. Electrochem. Soc. 154 (2007) B1200–B1205.